RESEARCH ARTICLE
doi: 10.2306/scienceasia1513-1874.2026.055

ScienceAsia 52 (3): 2026: ID 2026055: **1–10**

Mitochondrial respiration leak spurs chemoresistance in MT-ND5 mutant cybrids by suppressing mitophagy

Mohd Fazirul Mustafa[a], **Sharida Fakurazi**[a], **Maizaton Atmadini Abdullah**[b], **Sandra Maniam**[a,*]

[a] Department of Human Anatomy, Faculty of Medicine and Health Sciences, Universiti Putra Malaysia, 43400 UPM Serdang, Selangor Darul Ehsan, Malaysia

[b] Department of Pathology Faculty of Medicine and Health Sciences, Universiti Putra Malaysia, 43400 UPM Serdang, Selangor Darul Ehsan, Malaysia

*Corresponding author, e-mail: sandra@upm.edu.my

Received 7 Jun 2024, Accepted 17 Apr 2026
Available online 14 Jun 2026

ABSTRACT: Mitochondrial genomes have high mutation rate due to oxidative damage caused by reactive oxygen species (ROS). The gene encoding subunit 5 of complex I (ND5) was previously reported as a hotspot for mitochondrial DNA mutations in cancer tissues. This prompted us to investigate the role of ND5 mutation in cell proliferation, mitochondria bioenergetics, and cellular quality control that includes autophagy and mitophagy. Cybrid cell lines were developed using 3 commercial cell lines, CRL-1739, HGT-1 and MDA-MB-231 which harbour ND5 mutations. Cell proliferation was assessed through cell viability assays, and data on mitochondrial bioenergetics were obtained by measuring the oxygen consumption rate. Protein markers related to autophagy and mitophagy were evaluated using both immunoblotting and immunofluorescence. The cybrid lines showed significantly higher cell proliferation rate with significantly lower cell death compared to the negative control cells. The mitochondria bioenergetic assay reported an increase in basal respiration and proton leak but a decrease in spare respiratory capacity in cybrid cells compared to the negative control cells. The autophagy and mitophagy protein markers, were significantly decreased compared to negative control except the expression of BNIP-3. This study demonstrated that ND5 mutations resulted in increased proton leak which indicates increased ROS generation and mitochondrial dysfunction. The increased non-mitochondrial respiration is associated with altered metabolic intermediates that further promotes cancer cell viability and proliferation rate. The disruption of mitochondrial bioenergetics, which leads to accumulation of damaged mitochondria, may contribute to compromised cellular quality control, ultimately leading to tumorigenesis.

KEYWORDS: cancer, mitochondria, mitochondrial DNA, ND5 mutation, mitophagy, autophagy

INTRODUCTION

Several researchers have frequently reported the mitochondrial DNA (mtDNA) ND5 mutations at the m.13513G-A [1]. ND5 has been recognised as a hotspot in the study of pathogenesis mutations that affect complex I and often appears in a variety of clinical phenotypes ranging from single-organ dysfunctions to neurodegenerative disorders. For example, the genetic mutations of Leigh Syndrome (LS) are found at m.13051G-A, m.13094T-C, and m.12848T-C of the ND5 gene [2, 3]. Other pathogenic mutations identified in LS patients were found in mtDNA genes of complex I subunits, namely mitochondrial NADH dehydrogenase gene 3, ND3 (m.10191T>C), ND5 (m.12706T>C, m.13513G>A, m.13514T>C, and m.12338T>C), ND4 (m.11240C>T, m.11777C>A, and m.11778G>A), and ND6 (m.14459G>A, m.14439G>A, m.14502T>C, and m.12338T>C) [4, 5].

Another mitochondrial disorder with ND5 mutation is mitochondrial encephalomyopathy, lactic acidosis, and stroke-like episodes (MELAS). ND5 mutations were reported at m.1277A>G, m.13045A>C, m.13513G>A, and m.13514A>G in MELAS patients [6–8]. Interestingly, several ND5 mutations have also been associated with the combination of overlapping syndromes, including LS/MELAS (m.13513G-A and m.10197G-A) [9, 10], MELAS/ Myoclonic epilepsy with ragged red fibers (MERRF) (m.13042G-A, m.12147G-A, m.3243A-G and m.3252A-G) [11–14], Leber hereditary optic neuropathy (LHON)/MELAS (m.13042G-A and m.13513G-A) [15], and LS/MELAS/LHON (m.13513G-A) [16]. Studies have shown that ND5 were among the regions of mtDNA with more variants in at least half of the tumour samples of gastric cancer patients [17] and our lab has also identified ND5 as a hotspot for mutations associated in breast cancer tissue [18]. Currently, there are limited data on ND5 mutation and its pathogenic implication in cancer.

MtDNA is an integral part of the genetic landscape that drives the development and progression of various cancer. The mitochondrial autophagy (mitophagy) pathway is involved in the selective removal of damaged or dysfunctional mitochondria and represents a critical aspect of the metabolic restructuring that cancer cells undergo to meet their high bioenergetic demands. The aim of this study is to identify the effect of mitochondrial ND5 mutations on autophagy, mitophagy, cell viability, cell proliferation, and cell

oxidative stress in cancer cells using cybrid cell models.

MATERIALS AND METHODS

Cell culture

Human gastric carcinoma cells (CRL-1739 and HGT-1) and breast carcinoma cells (MCF-7 and MDA-MB-231) (ATCC, USA) were cultured as a monolayer in DMEM (HyClone, USA) supplemented with 100 µg/ml of streptomycin, 100 µg/ml of penicillin (BioWest, France), and 10% of Fetal Bovine Serum (FBS) (i-DNA, Malaysia). Cells were maintained at 37 °Cin 5% CO_2.

Treatment protocols

Chemicals were obtained commercially: Carbonyl cyanide 3-chlorophenylhydrazone (CCCP), rapamycin, and bafilomycin A1 from Sigma Aldrich, USA. To induce autophagy or mitophagy, cells were treated with either 20 mM of rapamycin or CCCP for 4 h. Autophagic flux in cells were inhibited by treating cells with bafilomycin A1 diluted in dimethyl sulfoxide (DMSO) to a final working concentration of 50 nM for 4 h.

Cybrid cell generation

The cybrid cell lines were developed according to the method by Vithayathil et al [19]. Three commercially available parental cell lines which include two gastric carcinoma cells (CRL-1739 and HGT-1) and one breast carcinoma cell (MDA-MB-231) were selected as they harbor ND5 mutations (Table S1). The cells were cultured in DMEM with high glucose concentration (4,500 mg/l) supplemented with 10% bovine serum albumin (BSA) and 1% penicillin/streptomycin.

The development of cybrid cell lines was performed through the fusion of enucleated parental cells (CRL-1739, HGT-1, and MDA-MB-231) with depleted mtDNA cells of MCF-7 by repeated treatment with EtBr [20]. The total depletion of mtDNA cells was then verified via PCR analysis. Next, the absence of nuclear DNA from the parental cells was confirmed by DNA gel electrophoresis, followed by Giemsa staining and Acridine Orange (AO)/Propidium Iodide (PI) (AOPI) staining for verification.

The cybrid populations forming single colonies were screened after 10–14 days. With continued growth, the cybrids were transferred to T25 flasks for the next 20 generations of culture to ensure that the nuclear-encoded mitochondrial proteins were incorporated into the newly introduced mitochondria.

Cell viability assay

The cytotoxicity of cybrid cells was determined by measuring the IC50 using the colorimetric cell viability assay as previously described by Mosmann [21]. Briefly, cells were plated into 96-well microplates at a density of 5×10^3 cells/well. The three cybrid cells were cultured at 37 °Cand treated at various time points (24–72 h) with 2.8 µM etoposide. 30 µl of MTT (3-(4,5-dimethylthiazol-2-yl)-2,5-diphenyltetrazolium bromide) solution (5 mg/ml) was added into each well, then incubated for 4 h in the dark. The formazan grains were dissolved in DMSO, and the absorbance at 570 nm (Wavelength range: 550– 600 nm) was read using an ELISA plate reader with the reference wavelength of higher than 650 nm.

Cell death analysis

Acridine orange/propidium iodide (AOPI) staining

Cell death in cybrid cells were detected using AOPI double staining and examined under fluorescence microscope. Briefly, treatment was performed on a 6-well plate. Cybrid cells were plated at a concentration of 1×10^6 cells/ml and treated with 2.8 µM etoposide. Cells were then incubated in 37 °Cin 5% CO_2 for 24, 48 and 72 h. The cells were trypsinised and collected into centrifuge tubes and centrifuged at 1,000×g for 10 min. In total, 10 µl fluorescent dyes, AO (10 µg/ml) and PI (10 µg/ml), were added into the cellular pellet at equal volumes. Freshly stained cell suspension was dropped onto a glass slide and covered with coverslip. Slides were observed under UV-Fluorescence microscope (Olympus, Japan) within 30 min prior to the fading of the fluorescence colour. The total number of viable cells was quantified in 5 different regions.

Cell proliferation assay

Briefly, cells were plated into 96-well microplates at a density of 5×10^3 cells/well. The three cybrid cells were cultured at 37 °Cand treated at various time points (24–72 h) with 2.8 µM etoposide. Bromodeoxyuridine (BrdU) (Cat. No: 2750, Sigma Aldrich) reagent was added into each well and incubated for 4 h. After incubation, the media was discarded, and 200 ml of fixing solution was added to fix the cells. The plate was incubated with anti-BrdU monoclonal antibody at room temperature for 1 h, followed by secondary antibody. The absorbance was measured at 450 nm using the ELISA plate reader, which represents the number of proliferation cells. The reference wavelength used was less than 650 nm.

Mitochondrial respiration based on the oxygen consumption rate (OCR)

Mitochondrial respiration was analysed using an Agilent Seahorse 96XF device (Agilent Technologies, USA) and respective kits. Cell mito stress test was performed as described in the manufacturer's protocol (Kit 103015–100). Briefly, cybrid cells were pre-treated, medium was exchanged for seahorse medium. Compounds were present during the entire measurement. Respiratory parameters, fuel dependency and capacity were calculated using the Seahorse Wave Desktop Software and the Seahorse XF Cell Mito Stress Test Report Generator.

Immunofluorescence staining

A total of 10,000 cells were seeded onto a sterile 6-well tissue culture plate attached with a round coverslip and coated with Type I collagen for 24 h. The coated coverslip cells were washed twice with PBS in 6-well plates, followed by fixation with 4% of paraformaldehyde for 20 min and permeabilisation with 0.1% of Triton X-100. After blocking with 2% BSA for 1 h, the cells were incubated overnight with anti-Beclin 1 (1:200), -LC3II (1 µg/ml), -BNIP-3 (1:150), -Parkin (1:200) primary antibodies at 4 °Cand washed thoroughly with PBS. Alexa-conjugated secondary antibodies (1: 1,000) are added and incubated for 1 h in the dark.

Immunoblot

Cell lysates were subjected to SDS-PAGE, and proteins were transferred to PVDF membranes (Thermo Fischer Scientific, USA). Membranes were blocked in PBS containing 5% non-fat milk and 0.1% Tween-20, washed twice in PBS containing 0.1% Tween-20, and incubated with anti-Beclin1 (1:1,000), -LC3II (0.5 µg/ml), -BNIP-3 (1:1,000), -Parkin (1:1,000) and -β-actin (1:1.000) primary antibodies and incubated overnight at 4 °C followed by the secondary antibody for 1 h at room temperature. Proteins of interest were visualized using the Enhanced Chemiluminescence (ECL) system (Thermo Fischer Scientific Pierce, USA). Densitometry analysis of protein bands was performed on Gel-Pro Analyzer software.

Statistical analysis

The collected data were analysed using the SPSS version 25.0 software. A paired sample t-test was used to determine the cell viability and cell proliferation rate between groups. The results were presented as the mean ± SEM. All p-values < 0.05 were considered statistically significant unless stated otherwise.

RESULTS

Cell viability is significantly enhanced in ND5 mutant cybrids

The effect of mitochondrial ND5 mutations on cell viability in cybrid cells (ND5mut-CRL, ND5mut-HGT, and ND5mut-MDA) treated with etoposide was assessed using the MTT assay (Fig. 1A). Notably, the cell viability of cybrid cells significantly increased compared to the negative control ($p < 0.05$) (Fig. 1A). However, it was consistently lower in all cybrid cells than in their respective parental cells (CRL-1739, HGT-1, and MDA-MB-231) ($p < 0.05$), and this trend was observed across all measured time points ($p < 0.05$) (Fig. 1A).

Morphological changes in the three cybrid cell lines (ND5mut-CRL, ND5mut-HGT, and ND5mut-MDA) treated with 2.8 µM etoposide were observed at 24, 48, and 72 h using AOPI staining (Fig. 1B). The percentage of cell viability in cybrid cells was significantly higher than the negative control ($p < 0.05$) but notably lower than the corresponding parental cell line ($p < 0.05$). The number of healthy cells decreased significantly over time (24, 48, and 72 h) in all etoposide-treated cells ($p < 0.05$) (Fig. 1B).

The proliferation rate of cybrid cell lines was assessed and compared to both the negative control and parental cells in the presence of etoposide (Fig. 1C). The percentage of cell proliferation for cybrid cells treated with etoposide was notably higher than the negative control ($p < 0.05$) but significantly lower than the corresponding parental cell line ($p < 0.05$) (Fig. 1C). Additionally, the proliferation rate of cells decreased significantly over time (24, 48, and 72 h) in all etoposide-treated negative cells ($p < 0.05$) (Fig. 1C).

Modulation of mitochondrial bioenergetics in ND5 mutant cybrids

In this study, 50,000 cells were seeded per well in replicates of three for all cell lines. Using a Seahorse XF96 flux analyzer, OXPHOS properties were measured according to OCR and parameters such as basal respiration, ATP production, proton leak, maximal respiration, spare respiratory capacity, and non-mitochondrial respiration were determined after successive injections of the ATP synthase inhibitor oligomycin (1.5 µM final concentration), the uncoupler carbonyl cyanide-4-(trifluoromethoxy)phenylhydrazone FCCP (0.25 µM final concentration), the complex I inhibitor rotenone and the complex III inhibitor antimycin A (50 µM final concentrations each) into the wells with seeded cells (Fig. 2A–Ci).

Interestingly, it was noted that both mutant ND5 in cybrid gastric lines (ND5mut-CRL and ND5mut-HGT) exhibited the highest basal respiration rate and spare respiratory capacity compared to the negative control ($p < 0.05$) (Fig. 2A(ii,vi) and 2B(ii,vi)). Although an increasing trend was noted in ND5mut-MDA, statistical significance was not achieved. From all the cybrid cell lines, ND5mut-CRL showed significantly higher ATP production compared to the negative control ($p < 0.05$) (Fig. 2Aiii). These responses, however, were not observed in ND5mut-HGT and ND5mut-MDA (Fig. 2Biii and 2Ciii). Additionally, while an increase in proton leak compared to the negative control was evident in all cybrid cells, statistical significance ($p < 0.05$) was only established in ND5mut-HGT cells (Fig. 2A–Civ). Maximal respiration, also known as peak OCR, is a measurement of the capacity of a cell to produce energy to meet its metabolic demands. Interestingly, no significant differences were seen in maximum respiration for all cybrids (ND5mut-CRL, ND5mut-HGT, and ND5mut-MDA) compared to the negative control (Fig. 2A–Cv). Non-mitochondrial respiration is a process that occurs in cells where oxygen is still consumed even after the addition of rotenone and antimycin A. The non-mitochondrial respiration was significantly higher in all cybrids compared to the

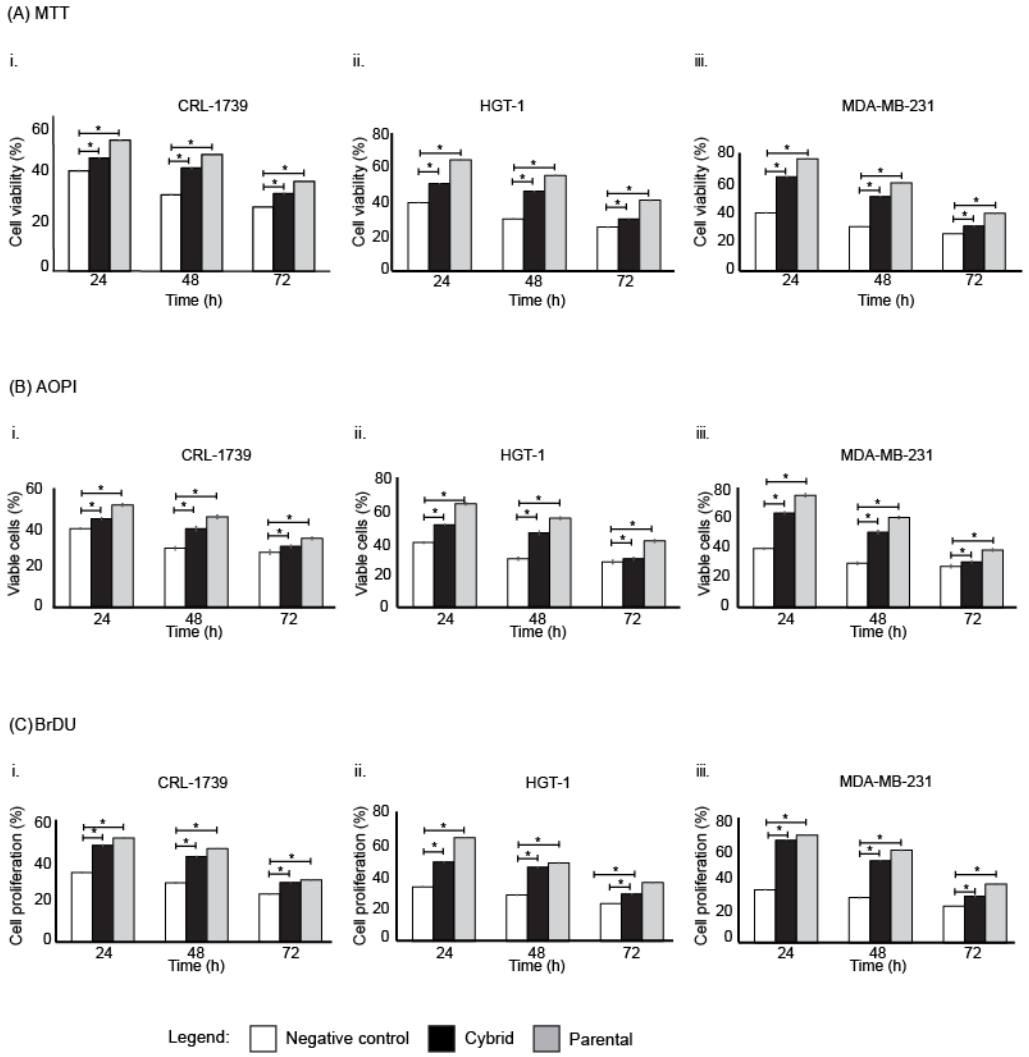

Fig. 1 Cell viability is significantly enhanced in ND5 mutant cybrids. Percentage of cell viability (A), AOPI staining (B) and BrDU labelling of 2.8 µM of etoposide treated ND5 mutant cybrid cells (ND5mut- CRL, ND5mut- HGT, and ND5mut-MDA) after 24, 48 and 72 h. MCF-7 cell line serves as a negative that does not harbour ND5 mutation and parental cells represent the wild-type cells of the respective cybrid cells. All data shown are the mean ± SD of three independent experiments. * $p < 0.05$ indicates a statistically significant difference compared to the negative control.

negative control ($p < 0.05$). (Fig. 2A–Cvii).

In summary, the data on mitochondrial bioenergetics suggest the mutant ND5 cybrids showed signs of mitochondrial dysfunction (increased proton leak and reduced spare respiratory capacity). The increase in basal respiration despite the lack of a significant difference in ATP production and maximal respiration, suggests that cybrids are rewiring their metabolic pathways to compensate for mitochondrial dysfunction (Table S1).

A decrease in autophagy and mitophagy in ND5 mutant cybrids

Autophagy and mitophagy are adaptive responses that can either promote cell survival by clearing damaged components or contribute to cell death by eliminating essential organelles under severe stress conditions. While mitophagy is generally considered a protective mechanism to remove dysfunctional mitochondria, excessive or dysregulated mitophagy may lead to the loss of healthy mitochondria, exacerbating mitochondrial dysfunction. The impact of ND5 mutations on autophagy and mitophagy activity was explored in ND5 mutant cybrid cells by examining the expression levels of key protein markers associated with autophagosome formation, namely LC3II, Beclin-1, (Fig. 3A–C(i,iv)) BNIP-3, and Parkin (Fig. 4A–C(i,iv), Table S2).

The protein expression of LC3II showed no significant difference in cells treated with rapamycin compared to negative control for all cybrid cells

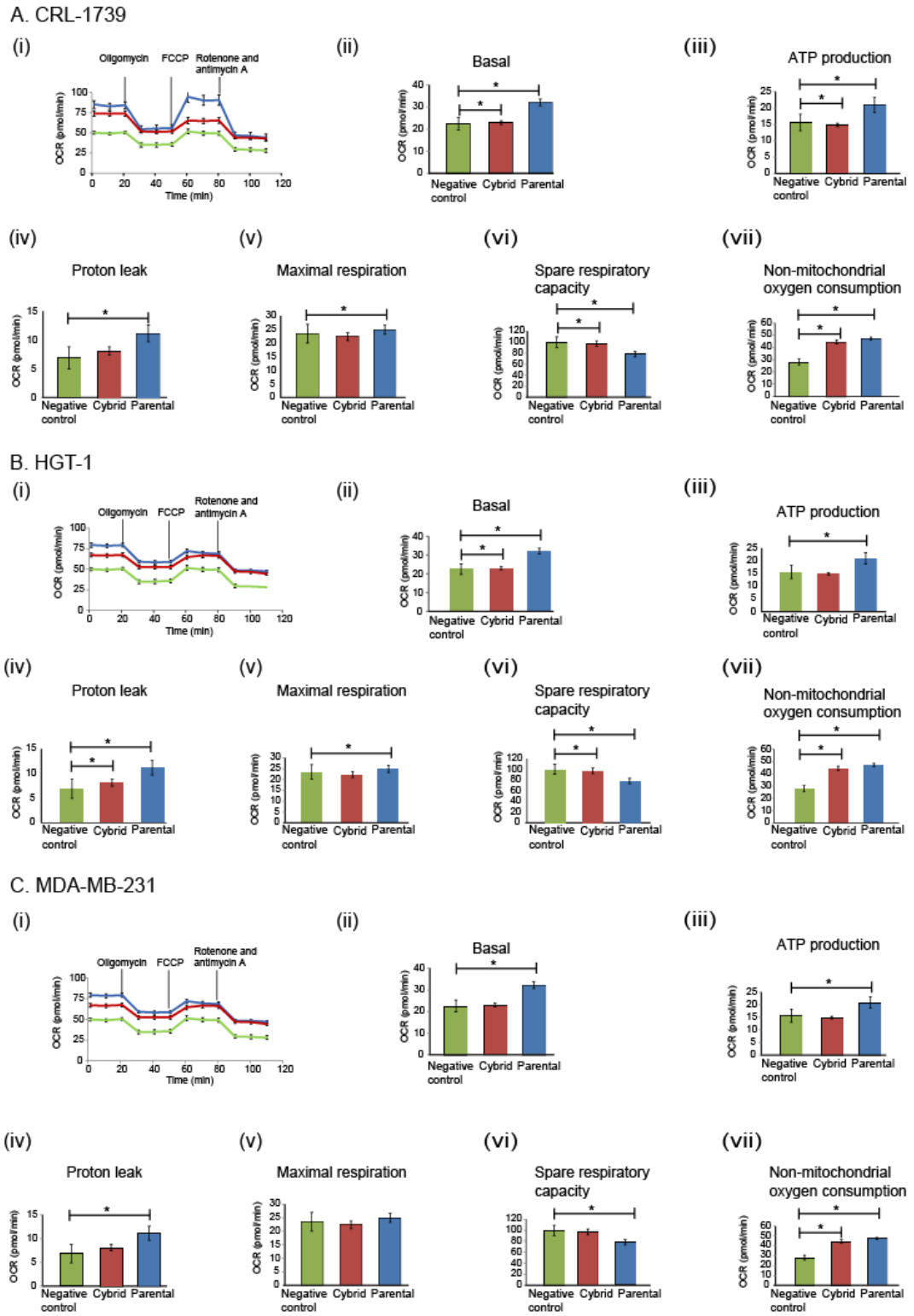

Fig. 2 Modulation of mitochondrial bioenergetics in ND5 mutant cybrids. The oxygen consumption rate (OCR) was measured using extracellular flux analysis (SeaHorse XF96) on monolayers of ND5 mutant cybrid cells (ND5mut- CRL, ND5mut- HGT, and ND5mut-MDA) for 2 h. Subsequently, ATP synthase inhibitor (oligomycin), mitochondrial uncoupler (CCCP), complex I inhibitor (rotenone), and complex III inhibitor (antimycin A) were added to determine the effects of ND5 mutations on mitochondrial respiration. MCF-7 cell line serves as a negative that does not harbour ND5 mutation and parental cells represent the wild-type cells of the respective cybrid cells. Each value represents the mean ± SEM, $n = 6$ for each experiment. * $p < 0.05$ indicates a statistically significant difference compared to the negative control.

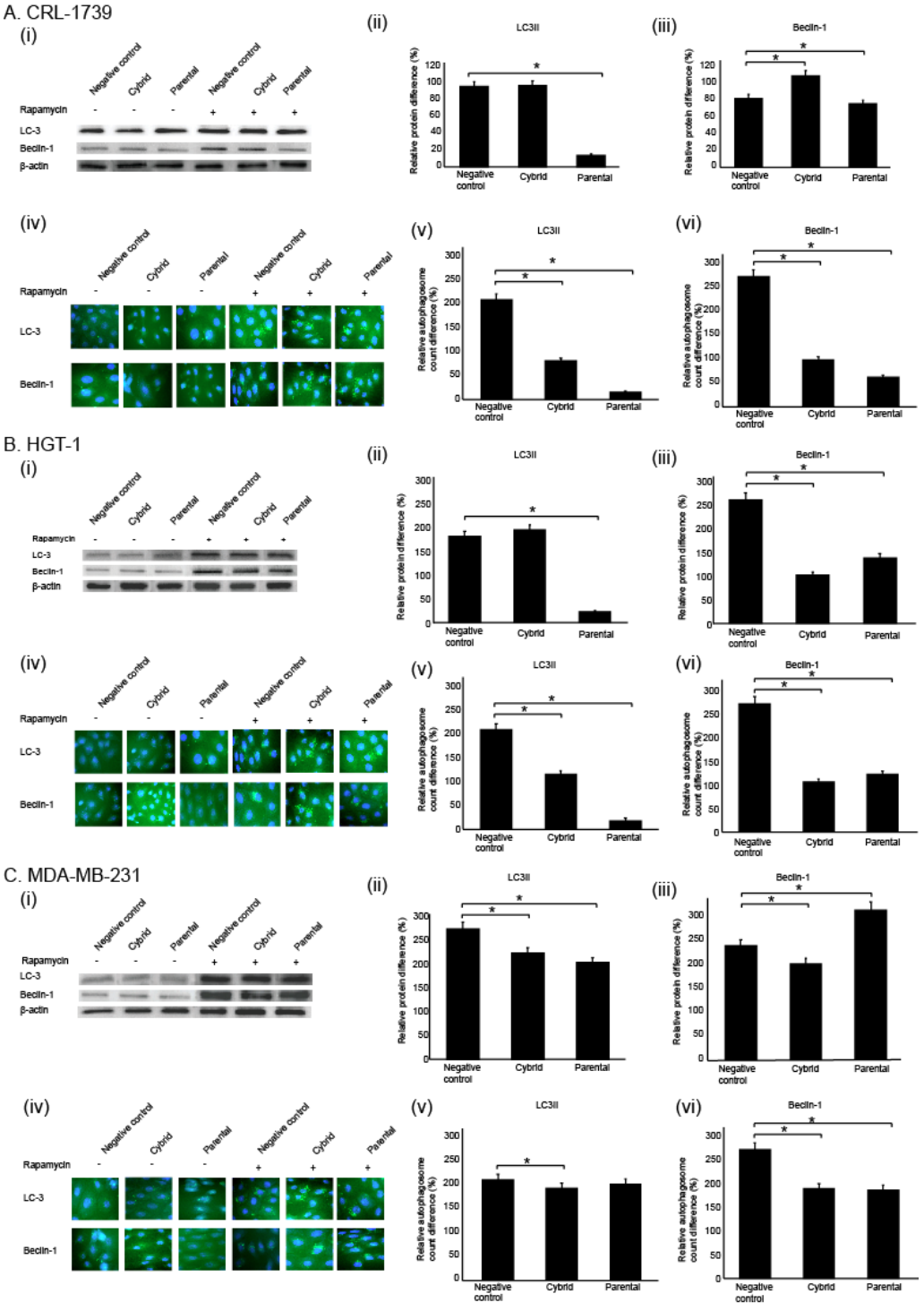

Fig. 3 A decrease in autophagy in ND5 mutant cybrids. Western blot of autophagic marker expression in ND5 mutant cybrid cells (ND5mut- CRL, ND5mut- HGT, and ND5mut-MDA) after treatment with 20 mM of rapamycin for 4 h. Cell lysates were subjected to immunoblotting with the indicated antibodies. β-actin was used as a loading control (i). The relative levels of LC3II (ii) and Beclin-1 (iii) expression was presented after normalization with loading control, (i–iii) Representative immunofluorescence images showing LC3 and Beclin 1 staining in all ND5 mutant cybrid cells; (iv) Quantification of the puncta average size and average number from the images in (iv) performed using ImageJ quantification tool (v–vi). Quantification performed from 3 experiments with > 25 cells quantified for each condition. MCF-7 cell line serves as a negative that does not harbour ND5 mutation and parental cells represent the wild-type cells of the respective cybrid cells. Error bars represent standard deviation (SD). $^*p < 0.05$ indicates a statistically significant difference compared to the negative control.

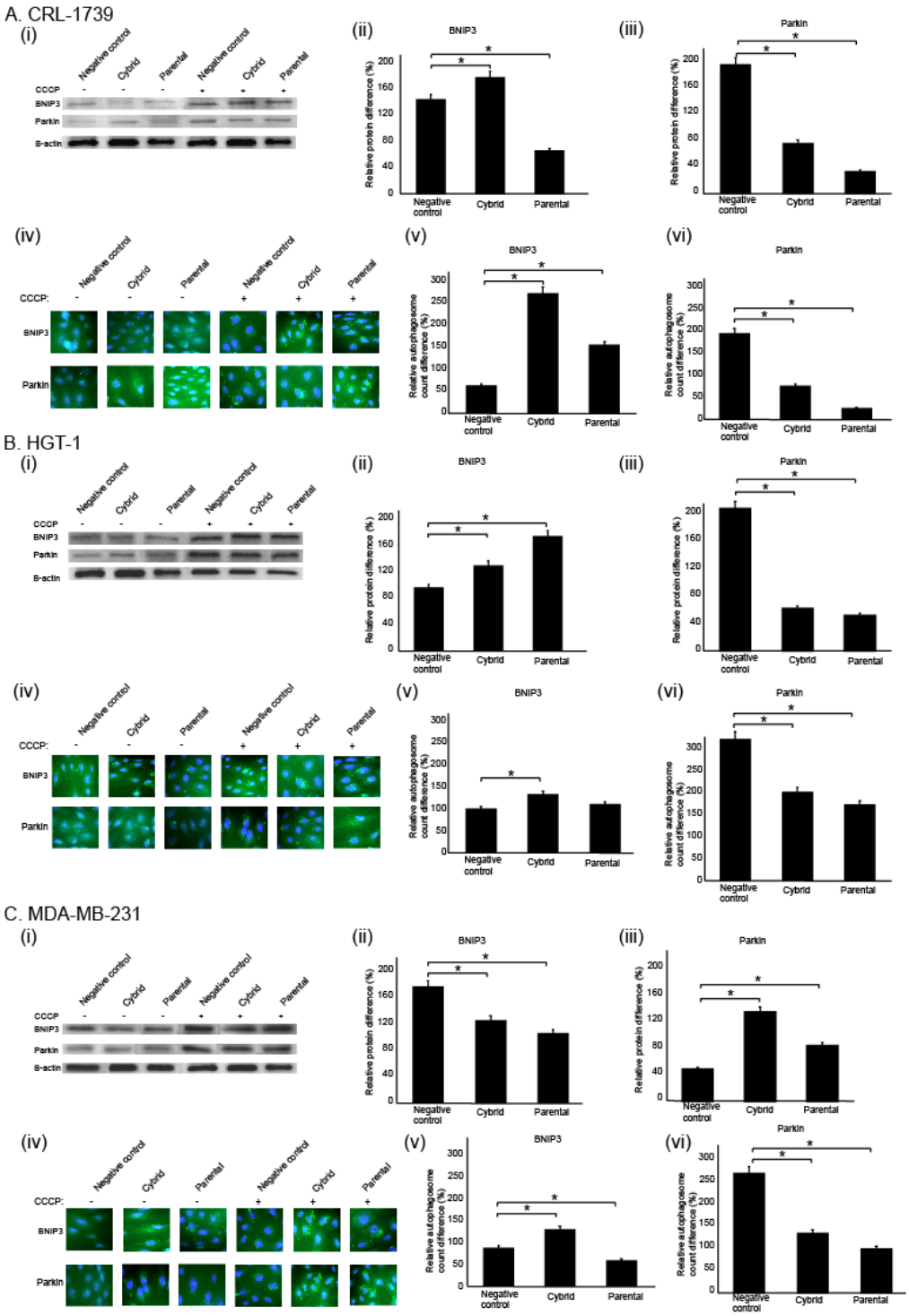

Fig. 4 A decrease in mitophagy in ND5 mutant cybrids. Western blot of mitophagy marker expression in ND5 mutant cybrid cells (ND5mut- CRL, ND5mut- HGT, and ND5mut-MDA) after treatment with 20 mM of CCCP for 4 h. Cell lysates were subjected to immunoblotting with the indicated antibodies. β-actin was used as a loading control (i). The relative levels of BNIP3 (ii) and Parkin(iii) expression was presented after normalization with loading control. Representative immunofluorescence images showing BNIP3 and Parkin staining in all ND5 mutant cybrid cells; (iv) Quantification of the puncta average size and average number from the images in (iv) performed using ImageJ quantification tool (v–vi). Quantification performed from 3 experiments with > 25 cells quantified for each condition. MCF-7 cell line serves as a negative that does not harbour ND5 mutation and parental cells represent the wild-type cells of the respective cybrid cells. Error bars represent SD. * $p < 0.05$ indicates a statistically significant difference compared to the negative control.

($p < 0.05$) (Fig. 3Aii,Bii) except for ND5mut-MDA (Fig. 3Cii). On the other hand, Beclin-1 expression significantly decreased in all cybrid cells treated with rapamycin compared to the negative control ($p < 0.05$) (Fig. 3Biii,Ciii), except for ND5mut-CRL (Fig. 3Aiii). In contrast to the immunoblotting data, more coherent data was obtained through IF analyses. A significant decrease in the expression of LC3II and Beclin-1 was consistently observed in all cybrid cells treated with rapamycin when compared to the negative control ($p < 0.05$) (Fig. 3A–C(v,vi)).

There was a significant increase in the BNIP-3 protein expression in both ND5mut-CRL and ND5mut-HGT cells treated with CCCP compared to the negative control (($p < 0.05$) (Fig. 4Aii,Bii). Conversely, the two cybrid cells (ND5mut-CRL and ND5mut-HGT) showed a significant decrease in the Parkin expression in cells treated with CCCP compared to the negative control ($p < 0.05$) (Fig. 4,Biii). Unlike the immunoblotting data, the IF findings exhibited a more uniform observation. In all cybrid cells treated with CCCP, there was a significant increase in BNIP-3 expression ($p < 0.05$) (Fig. 4A–C v) and a decrease in Parkin expression ($p < 0.05$) (Fig. 4A–Cvi) compared to the negative control.

DISCUSSION

Mitochondria play a critical role in the regulation of cell growth and survival, and their dysfunction can lead to the development and progression of cancer [22]. One of the key functions of mitochondria is to produce ATP through oxidative phosphorylation. When mitochondria are dysfunctional, energy production is impaired, leading to an altered energy metabolism in cancer cells which is characterised by a shift towards aerobic glycolysis (the Warburg effect), that allows cancer cells to generate ATP even in the absence of oxygen [23, 24]. Mitochondria generate ROS as a by-product of oxidative phosphorylation, and excessive ROS production can lead to oxidative damage to DNA, proteins, and lipids inducing mutations and chromosomal abnormalities, leading to genomic instability and increased risk of cancer development [25]. Mutations in mtDNA have been observed in many cancers, and alterations in mitochondrial function have been associated with drug resistance and poor prognosis in cancer patients.

Three commercially available cancer cell lines with reported ND5 mutations; CRL-1739 [26], HGT-1, and MDA-MD-231 [27] (Table S1) were chosen for cybrid cell line development. The cybrid model is cost-effective *in vitro* system that expresses selected mtDNA with fixed nuclear DNA background. It serves as a useful tool for studying the effects of ND5 mutations on cell physiology and cancer development. The effects of mitochondrial ND5 mutations on autophagy, mitophagy, cell viability, cell proliferation, and cell oxidative stress in cancer cells were explored using cybrid cell models. The data from this study indicates that ND5 mutation plays a significant role in chemoresistance and proliferation of cybrid cells. The results of the MTT assay and BrdU assay showed that the cybrid cells exhibit significantly higher cellular viability and cellular proliferation rates with significantly lower cell death than the negative control cells (MCF-7) which are devoid of ND5 mutation (Fig. 1A,C). The chemoresistance observed in cybrid cells was postulated due to increased ROS production which is supported by the findings from the mitochondrial bioenergetic assay. An increase in basal respiration and proton leak and a decrease in spare respiratory capacity in cybrid cells suggest the presence of a compensatory response to the loss of mitochondrial respiratory chain efficiency (Table S1). The disruption of the electrochemical gradient created by the movement of protons impairs the ability of the respiratory chain to generate ATP [28–30]. The increase in proton leak leads to the production of mtROS, which can damage mitochondrial proteins, lipids, and DNA [31]. This damage, in turn, can impair mitochondrial function and contribute to increased cancer cell proliferation.

Autophagy and mitophagy are cellular processes that help maintain cellular homeostasis and regulate the turnover of damaged or dysfunctional organelles. Both processes play an important role in tumour progression, and their dysregulation can contribute to cancer development [32–36]. Autophagy has a dual role in cancer, and its role can be tumour-suppressive or tumour-promoting, depending on the stage of cancer development [37, 38]. In the early stages of tumour development, autophagy can suppress tumour formation by removing damaged or mutated organelles and preventing DNA damage. However, in advanced tumour stages, autophagy can promote tumour growth by providing nutrients and energy to the tumour cells, enhancing their survival under stress conditions, and promoting tumour cell invasion and metastasis. Cybrid cells exhibit decreased expression of autophagy protein markers; LC3II and Beclin-1, indicating reduced autophagy activity compared to the negative control (Table S2).

An increase in BNIP-3 with a decrease in Parkin expression in cybrid cells compared to the negative control was noted (Table S2). ND5 mutations were found to significantly impair the recruitment of Parkin to damaged mitochondria despite an increase in BNIP3 which suggests an active role of ND5 in initiating the mitophagy process. The decreased Parkin expression in the cybrid cells leads to restricted autophagosome formation. This could be explained by poor recruitment of E1 enzyme Atg7 to the damaged mitochondria which is essential for LC3II production and the assembly functional autophagosomes [39]. These findings are consistent with our findings of lower levels of LC3II in the cybrid cells compared to the negative control. This suggests that the ND5 mutations contribute to the inability of recognition and ubiquitination of Parkin-

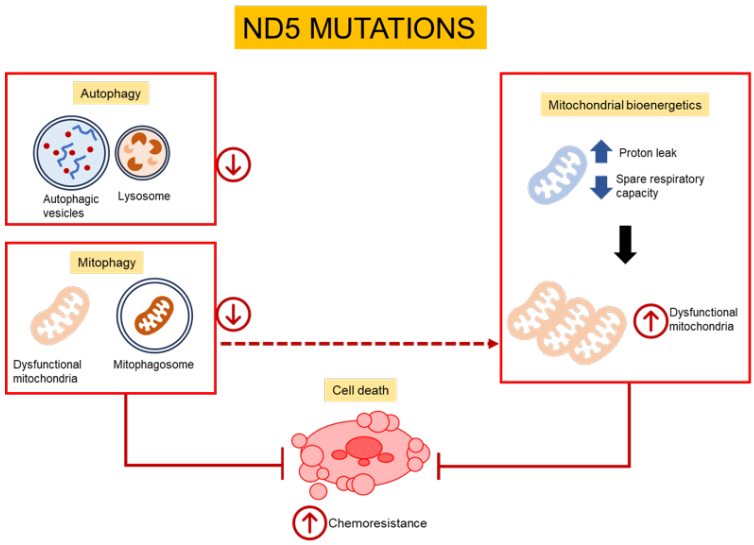

Fig. 5 Schematic summarising the role of ND5 mutations in cancer cell chemoresistance. ND5 mutations drive mitochondrial dysfunction, increased ROS production, metabolic reprogramming, and enhanced cell proliferation. Disrupted autophagy and impaired Parkin-mediated mitophagy lead to mitochondrial stress and reduced respiratory chain efficiency.

damaged mitochondrial proteins. Consequently, this could result in cellular stress and a decline in the efficiency of the mitochondrial respiratory chain.

The data presented in this study suggest that ND5 mutations play a significant role in the chemoresistance and proliferation of cancer cells (Fig. 5). The increased cell viability and proliferation rate observed in cancer cells is due to increased ROS production resulting from mitochondrial dysfunction (Fig. 5). This in turn contributes to the rewiring of cellular metabolism. ND5 mutations were also found to play a role in the dysregulation of autophagy activity in cancer cells. The effect of ND5 mutations on mitophagy suggests that it contributes to the inability to recognise and ubiquitinate Parkin-damaged mitochondrial proteins, leading to cellular stress and reduced mitochondrial respiratory chain efficiency. The findings of this study provide valuable insights into the molecular mechanisms underlying the role of ND5 mutations in cancer progression and mitochondrial dysfunction in cancer cells.

Appendix A. Supplementary data

Supplementary data associated with this article can be found at https://dx.doi.org/10.2306/scienceasia1513-1874.2026.055.

Acknowledgements: This work was supported by the Ministry of Education Malaysia (Programme Grant: Fundamental Research Grant Scheme FRGS/1/2015/SKK02/UPM/02/4) and Universiti Putra Malaysia (Programme Grant: Putra Grant GP-IPS/2017/9576800). MF Mustafa was supported by Graduate Research Fellowship from Universiti Putra Malaysia.

REFERENCES

1. Sudo A, Honzawa S, Nonaka I, Goto Y (2004) Leigh syndrome caused by mitochondrial DNA G13513A mutation: Frequency and clinical features in Japan. *J Hum Genet* **49**, 92–96.
2. Dombi E, Dio A, Morten K, Carver J, Lodge T, Fratter C, Ng YS, Liao C, et al (2016) The m.13051G>A mitochondrial DNA mutation results in variable neurology and activated mitophagy. *Neurology* **86**, 1921–1923.
3. Emperador S, Vidal M, Hernández-Ainsa C, Ruiz-Ruiz C, Woods D, Morales-Becerra A, Arruga J, Artuch R, et al (2018) The decrease in mitochondrial DNA mutation load parallels visual recovery in a Leber hereditary optic neuropathy patient. *Front Neurosci* **12**, 61.
4. Yu XL, Yan CZ, Ji KQ, Lin PF, Xu XB, Dai TJ, Li W, Zhao YY (2018) Clinical, neuroimaging, and pathological analyses of 13 Chinese Leigh syndrome patients with mitochondrial DNA mutations. *Chin Med J* **131**, 2705–2712.
5. Xu B, Li X, Du M, Zhou C, Fang H, Lyu J, Yang Y (2017) Novel mutation of ND4 gene identified by targeted next-generation sequencing in a patient with Leigh syndrome. *J Hum Genet* **62**, 291–297.
6. Lorenzoni PJ, Werneck LC, Kay CSK, Silvado CES, Scola RH (2015) When should MELAS (mitochondrial myopathy, encephalopathy, lactic acidosis, and stroke-like episodes) be the diagnosis? *Arq Neuropsiquiatr* **73**, 959–967.
7. Liolitsa D, Rahman S, Benton S, Carr LJ, Hanna MG (2003) Is the mitochondrial complex I ND5 gene a hotspot for MELAS-causing mutations? *Ann Neurol* **53**, 128–132.
8. Wang Z, Qi XK, Yao S, Chen B, Luan X, Zhang W, Han M, Yuan Y (2010) Phenotypic patterns of MELAS/Leigh syndrome overlap associated with m.13513G>A mutation and neuropathological findings in one autopsy case. *Neuropathology* **30**, 606–614.

9. Brusa R, Mauri E, Dell'Arti L, Magri F, Ronchi D, Minorini V, Mainetti C, Gagliardi D, et al (2020) Expanding the clinical spectrum of the mitochondrial mutation A13084T in the ND5 gene. *Neurol Genet* **6**, e511.
10. Leng Y, Liu Y, Fang X, Li Y, Yu L, Yuan Y, Wang Z (2015) The mitochondrial DNA 10197G>A mutation causes MELAS/Leigh overlap syndrome presenting with acute auditory agnosia. *Mitochondrial DNA* **26**, 208–212.
11. Tan YY, Tee TY, Chew FY, Kok HT, Rani NHA, Ngu LH, Viswanathan S (2023) Mitochondrial DNA 3252A>G mutation presenting as MERRF/MELAS overlapping syndrome: A case report. *Neurol Asia* **28**, 1073–1076.
12. Melone MAB, Tessa A, Petrini S, Lus G, Sampaolo S, di Fede G, Santorelli FM, Cotrufo R (2004) Revelation of a new mitochondrial DNA mutation (G12147A) in a MELAS/MERRF phenotype. *Arch Neurol* **61**, 269–272.
13. Naini AB, Lu J, Kaufmann P, Bernstein RA, Mancuso M, Bonilla E, Hirano M, DiMauro S (2005) Novel mitochondrial DNA ND5 mutation in a patient with clinical features of MELAS and MERRF. *Arch Neurol* **62**, 473–476.
14. Nakamura M, Nakano S, Goto Y, Ozawa M, Nagahama Y, Fukuyama H, Akiguchi I, Kaji R, Kimura J (1995) A novel point mutation in the mitochondrial tRNASer(UCN) gene detected in a family with MERRF/MELAS overlap syndrome. *Biochem Biophys Res Commun* **214**, 86–93.
15. Sun CB, Bai HX, Xu DN, Xiao Q, Liu Z (2021) Mitochondrial 13513G>A mutation with low mutant load presenting as isolated Leber's hereditary optic neuropathy assessed by next-generation sequencing. *Front Neurol* **12**, 601307.
16. Blok MJ, Spruijt L, de Coo IF, Schoonderwoerd K, Hendrickx A, Smeets HJ (2007) Mutations in the ND5 subunit of complex I of the mitochondrial DNA are a frequent cause of oxidative phosphorylation disease. *J Med Genet* **44**, e74.
17. Cavalcante GC, Ribeiro-dos-Santos Â, de Araújo GS (2022) Mitochondria in tumour progression: A network of mtDNA variants in different types of cancer. *BMC Genom Data* **23**, 1–10.
18. Omasanggar R, Yu CY, Ang GY, Emran NA, Kitan N, Baghawi A, Ahmad AF, Abdullah MA, et al (2020) Mitochondrial DNA mutations in Malaysian female breast cancer patients. *PLoS One* **15**, e0233461.
19. Vithayathil SA, Ma Y, Kaipparettu BA (2012) Transmitochondrial cybrids: Tools for functional studies of mutant mitochondria. *Methods Mol Biol* **837**, 219–230.
20. Naito A, Carcel-Trullols J, Xie C, Evans TT, Mizumachi T, Higuchi M (2008) Induction of acquired resistance to antiestrogen by reversible mitochondrial DNA depletion in breast cancer cell line. *Int J Cancer* **122**, 1506–1511.
21. Mosmann T (1983) Rapid colorimetric assay for cellular growth and survival: Application to proliferation and cytotoxicity assays. *J Immunol Methods* **65**, 55–63.
22. Wang SF, Tseng LM, Lee HC (2023) Role of mitochondrial alterations in human cancer progression and cancer immunity. *J Biomed Sci* **30**, 1–19.
23. Martins Pinto M, Paumard P, Bouchez C, Ransac S, Duvezin-Caubet S, Mazat JP, Rigoulet M, Devin A (2023) The Warburg effect and mitochondrial oxidative phosphorylation: Friends or foes? *Biochim Biophys Acta Bioenerg* **1864**, 148931.
24. Cassim S, Vučetić M, Ždralević M, Pouyssegur J (2020) Warburg and beyond: The power of mitochondrial metabolism to collaborate or replace fermentative glycolysis in cancer. *Cancers* **12**, 1119.
25. Hanahan D, Weinberg RA (2011) Hallmarks of cancer: The next generation. *Cell* **144**, 646–674.
26. Li L, Xing R, Cui J, Li W, Lu Y (2018) Investigation of frequent somatic mutations of MTND5 gene in gastric cancer cell lines and tissues. *Mitochondrial DNA B* **3**, 1004–1010.
27. Imanishi H, Hattori K, Wada R, Ishikawa K, Fukuda S, Takenaga K, Nakada K, Hayashi JI (2011) Mitochondrial DNA mutations regulate metastasis of human breast cancer cells. *PLoS One* **6**, e23401.
28. Layec G, Blain GM, Rossman MJ, Park SY, Hart CR, Trinity JD, Gifford JR, Sidhu SK, et al (2018) Acute high-intensity exercise impairs skeletal muscle respiratory capacity. *Med Sci Sports Exerc* **50**, 2409–2417.
29. Cheng J, Nanayakkara G, Shao Y, Cueto R, Wang L, Yang WY, Tian Y, Wang H, Yang X (2017) Mitochondrial proton leak plays a critical role in pathogenesis of cardiovascular diseases. *Adv Exp Med Biol* **982**, 359–370.
30. Chelimsky G, Simpson P, Zhang L, Bierer D, Komas S, Kalyanaraman B, Chelimsky T (2021) Impaired mitochondrial bioenergetics function in pediatric chronic overlapping pain conditions with functional gastrointestinal disorders. *Pain Res Manag* **2021**, 6627864.
31. Juan CA, de la Lastra JMP, Plou FJ, Pérez-Lebeña E (2021) The chemistry of reactive oxygen species (ROS) revisited. *Int J Mol Sci* **22**, 4642.
32. Rakesh R, PriyaDharshini LC, Sakthivel KM, Rasmi RR (2022) Role and regulation of autophagy in cancer. *Biochim Biophys Acta Mol Basis Dis* **1868**, 166400.
33. Vitto VAM, Bianchin S, Zolondick AA, Pellielo G, Rimessi A, Chianese D, Yang H, Carbone M, et al (2022) Molecular mechanisms of autophagy in cancer development, progression, and therapy. *Biomedicines* **10**, 1596.
34. Nazio F, Bordi M, Cianfanelli V, Locatelli F, Cecconi F (2019) Autophagy and cancer stem cells: Molecular mechanisms and therapeutic applications. *Cell Death Differ* **26**, 690–702.
35. Denisenko TV, Gogvadze V, Zhivotovsky B (2021) Mitophagy in carcinogenesis and cancer treatment. *Discov Oncol* **12**, 1–11.
36. Chang JY, Yi HS, Kim HW, Shong M (2017) Dysregulation of mitophagy in carcinogenesis and tumor progression. *Biochim Biophys Acta Bioenerg* **1858**, 633–640.
37. Yun CW, Lee SH (2018) The roles of autophagy in cancer. *Int J Mol Sci* **19**, 3466.
38. Kwantwi LB (2024) The dual role of autophagy in the regulation of cancer treatment. *Amino Acids* **56**, 1–7.
39. Zuo H, Chen C, Sa Y (2023) Therapeutic potential of autophagy in immunity and inflammation: Current and future perspectives. *Pharmacol Rep* **75**, 499–510.

Appendix A. Supplementary data

Table S1 Mitochondrial bioenergetics in ND5 mutant cybrids.

Mitochondrial bioenergetics	Effect on OCR		
	ND5mut-CRL	ND5mut-CRL	ND5mut-CRL
Basal respiratory	Increased	Increased	Increased
ATP production	Increased	No diff	No diff
Proton leak	Increased[#]	Increased	Increased[#]
Maximal respiratory	No diff	No diff	No diff
Spare respiratory capacity	Decreased	Decreased	Decreased[#]
Non-mitochondrial respiratory	Increased	Increased	Increased

[#] indicates not statistically significant; No diff = No difference.

Table S2 The protein expression of autophagy and mitophagy markers in ND5 mutant cybrids compared to negative control.

Cybrid cell	Autophagy marker				Mitophagy marker			
	LC3II		Beclin 1		BNIP-3		Parkin	
	Immunoblot	IF	Immunoblot	IF	Immunoblot	IF	Immunoblot	IF
ND5mut-CRL	No diff	Decreased	Increased	Decreased	Increased	Increased	Decreased	Decreased
ND5mut-HGT	No diff	Decreased	Decreased	Decreased	Increased	Increased	Decreased	Decreased
ND5mut-MDA	Decreased	Decreased	Decreased	Decreased	Decreased	Increased	Increased	Decreased

IF = Immunofluorescence; No diff = No difference.